

# Construction of Polyhedra with Tetravalent Nodes as an Analogue to Graphitic Systems

Hou-Hsun Ho<sup>1</sup>, Yung-Hsi Chang<sup>2</sup>, Chern Chuang<sup>3</sup>, and Bih-Yaw Jin<sup>4</sup>

<sup>1</sup>Department of Chemistry, National Taiwan University, Taipei, Taiwan; d10223105@ntu.edu.tw

<sup>2</sup>Department of Chemistry, National Taiwan University, Taipei, Taiwan; r10223184@ntu.edu.tw

<sup>3</sup>Dept. of Chem. and Biochem., University of Nevada, LV, NV, USA; chern.chuang@unlv.edu

<sup>4</sup>Department of Chemistry, National Taiwan University, Taipei, Taiwan; byjin@ntu.edu.tw

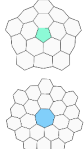
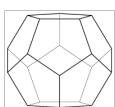
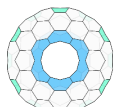
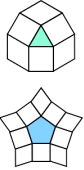
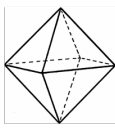
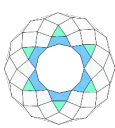
## Abstract

We study tetravalent analogues to fullerene systems which include Goldberg polyhedra (genus 0) and toroidal polyhedra (genus 1), where each node is connected to four others. According to the Euler-Poincaré formula, a tetravalent polyhedron with genus 0 has exactly 8 triangles, while on a toroidal polyhedron, the number of triangles and pentagons must be equal. We develop a construction method for toroidal polyhedra using a methodology similar to our previous work, which categorizes tetravalent toroidal polyhedra with a set of five indices. Bead models of the tori are presented as well.

## Introduction

Regular planar tilings, also known as Platonic tilings, are fascinating mathematical objects that have been studied for millennia. These tilings consist of three types: the equilateral triangle tiling, the square tiling, and the hexagonal tiling. In our previous work [3][4], we focused on characterizing trivalent systems and designing various hypothetical structures, such as fullerenes and carbon nanotubes of different shapes and topologies, by manipulating nonhexagonal defects in hexagonal tilings and applying suitable boundary conditions.

In this article, we aim to extend our previous work [3] by applying our methods to a square lattice, which is a tetravalent system. A comparison between trivalent and tetravalent systems is given in Figure 1. Positive and negative disclinations (topological defects) in trivalent systems are associated with pentagons and heptagons, respectively, while in tetravalent systems they are linked to triangles and pentagons, respectively.

Valency	Lattice	Defects	Polyhedron (genus 0)	Torus (genus 1)
 Trivalent	 Hexagonal		 $F_5 = 12$	 $F_5 = F_7$
 Tetravalent	 Square		 $F_3 = 8$	 $F_3 = F_5$

**Figure 1:** Comparison between trivalent and tetravalent systems. The defects of trivalent systems are pentagon and heptagon, respectively, while triangle and pentagon correspondences are seen in tetravalent systems. The Euler-Poincaré formula determines the number of  $n$ -gons, denoted by  $F_n$ , in both systems.

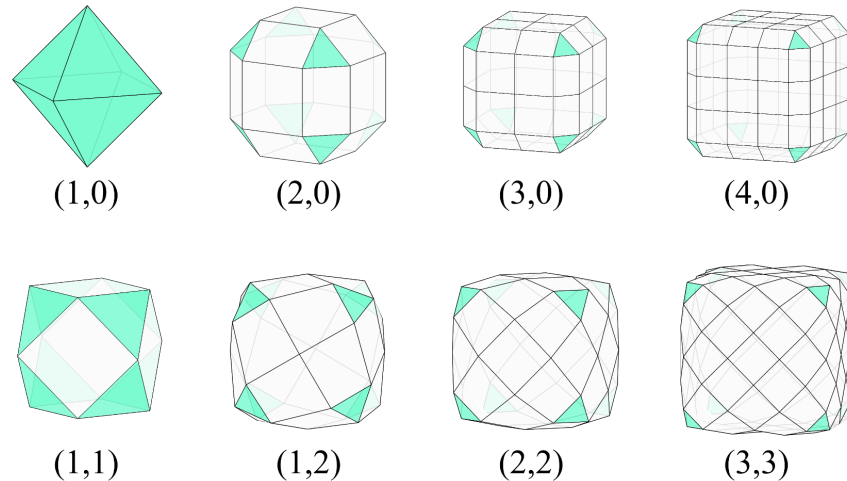


**Figure 2:** *The tetraivalent Goldberg polyhedra. Each polyhedron contains 8 triangles, and the indices are the vectors between two nearest triangles.*

A 3d polyhedron must meet the Euler-Poincaré formula, which establishes a relationship between its numbers of vertices  $V$ , edges  $E$ , faces  $F$ , and the genus  $g$ , as given by  $V - E + F = 2 - 2g$ . For a genus 0 polyhedron with trivalent vertices, if all the faces have 5 or 6 sides, there must be exactly 12 pentagons. Similarly, for a tetraivalent genus 0 polyhedron, it has 8 triangular faces if all the faces have 3 or 4 sides.

### Geometrical Constructions of Tetraivalent Polyhedra

The structures of genus 0 tetraivalent systems resemble those of trivalent fullerenes. Among numerous possibilities, we concentrate on ones with octahedral rotational symmetry, as they exhibit Goldberg polyhedral features which were discussed in [2], [5], and [6]. To classify a tetraivalent Goldberg polyhedron, we use a Goldberg vector represented by  $(h, k)$ , as described in [2]. This vector indicates the relative positions of the nearest triangles: first take  $h$  steps in one direction, then turn  $90^\circ$  to the left and take  $k$  steps, which is similar to the classification of trivalent Goldberg polyhedrons. Figure 2 displays several examples of tetraivalent Goldberg polyhedra with varying indices. Of particular note,  $(h, k) = (1, 0)$  corresponds to a regular octahedron, the  $(1, 1)$  configuration is equivalent to a cuboctahedron, and the  $(2, 0)$  configuration is a rhombicuboctahedron.

When it comes to tetraivalent toroidal structures, we have developed a construction scheme based on our previous research on their trivalent counterparts [3] adjusted to ensure compatibility with the new system's geometric characteristics. As a brief summary of the construction scheme used in [3], we will highlight the key steps and modifications made to fit the tetraivalent system.

To create a torus, multiple tube junctions must be connected consecutively. We illustrate the process of mitering tubes in Figure 3. Figure 3(a) shows a planar precursor to the tube in Figure 3(b), which is rolled up along the boundary vector  $\vec{T'T} = \vec{c} = (c_1, c_2)$  in (a). By specifying a chiral ( $c_1 \neq c_2$ ) boundary vector (in this case,  $\vec{c} = (2, 7)$ ), we can define a grey area that represents the mitered section using the vector and its achiral components  $(2, 2)$  and  $(0, 5)$ . T and P mark the locations where a triangle and a pentagon, respectively, will emerge in the final tube assembly in Figure 3(c). By cutting off the grey area in Figure 3(b) and connecting the tube segment to its mirror image counterpart at the cut surface, the handedness of the tube is flipped due to the impact of positive and negative defects, resulting in the junction in Figure 3(c).

Adapting a methodology akin to the one utilized in trivalent systems [3], we introduce two parameters, vertical shift ( $vs$ ) and horizontal shift ( $hs$ ), which define the linearly independent movements of the second

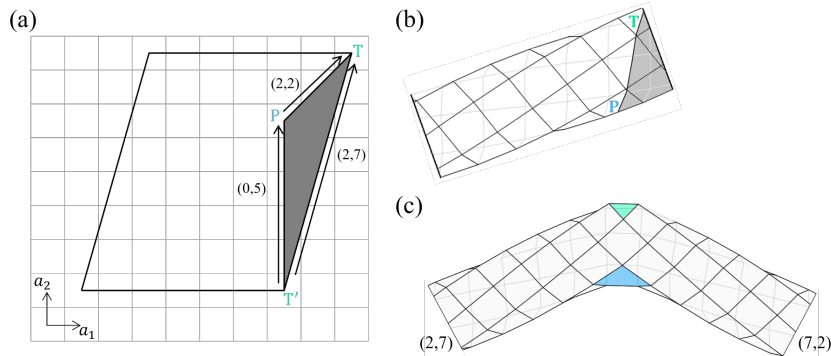


**Figure 3:** The process of mitering tetravalent tubes. (a) A planar precursor of tube (b). The grey area is defined by the boundary vector  $(2,7)$  and its achiral components  $(2,2)$  and  $(0,5)$ . (b) A tetravalent tube with the grey area to be cut off during the mitering process. (c) A mitered tube with a pair of triangle and pentagon connecting mirror-imaged tubes  $(7,2)$ - $(2,7)$ .

junction in a mitered tube relative to the first junction. A comprehensive definition of these parameters is available in [3].

Possible positions of the second junction, parametrized by  $(vs, hs)$ , are shown in Figure 4(a). Positions with identical  $hs$  values are marked using the same greyscale. However, it is worth noting that in tetravalent systems, the parameter  $vs$  ranges from 1 to  $n$ , which differs from trivalent systems where the range is from 1 to  $n + m$ , due to the differences in the inner products of their lattice vectors. Meanwhile, the criteria for  $hs$  remains the same as in the trivalent system, which is  $0 \leq hs$ .

Using the parameters defined above and following the procedure outlined in Figure 3 of [3], we are able to construct a tetravalent structure with five indices  $(c_1, c_2, vs, hs, n_r)$ . Take the example of  $(c_1, c_2, vs, hs, n_r) = (7, 2, 4, 0, 3)$ , shown in Figure 4(b). In this structure,  $(7,2)$ - $(2,7)$  represents the boundary vectors of the junctioned tubes,  $(4,0)$  corresponds to the  $(vs, hs)$  pair, and  $n_r = 3$  indicates the number of times the mitering process is repeated as well as the rotational symmetry number of the final torus. Additional information and a more detailed discussion of the construction can also be found in [3].

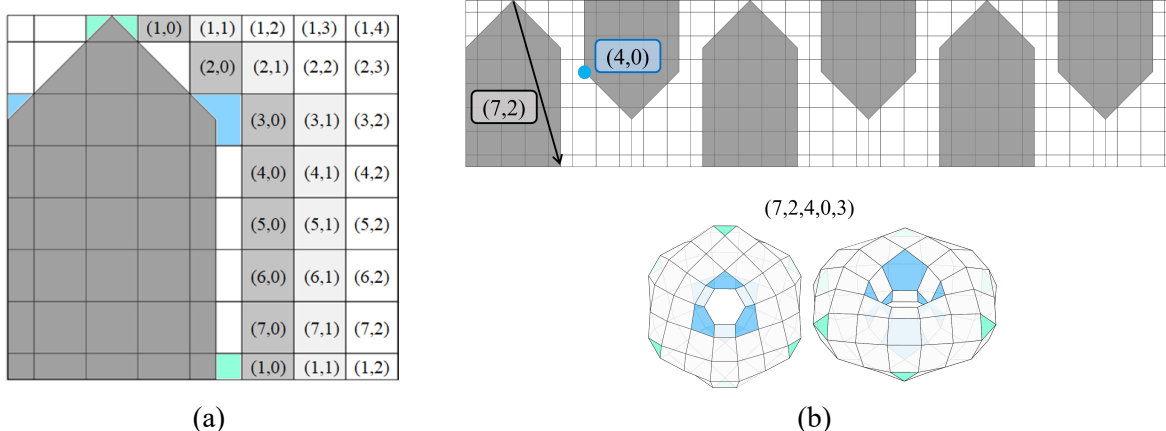


**Figure 4:** Parameters characterizing a tetravalent torus. (a) Possible positions of the second joint  $(vs, hs)$ . Positions with identical  $hs$  value are marked with the same greyscale. (b) A tetravalent torus with indices  $(c_1, c_2, vs, hs, n_r) = (7, 2, 3, 0, 4)$ . The torus below is constructed by cutting off the grey area of the upper sheet and glue the boundary sides of the remaining (white) sheet carefully [3].

### Bead Models of Tetravalent Toroidal Polyhedra

With the strategy elaborated above, we present several examples of tetravalent toroidal polyhedron in Figure 5. Here the computer-generated structures are shown in the upper panel and corresponding bead models are shown in the lower panel. The beads represent the positions of the edges in a polyhedron. Color beads indicate edges of the triangular and pentagonal faces of the polyhedron, while all other beads remain white.

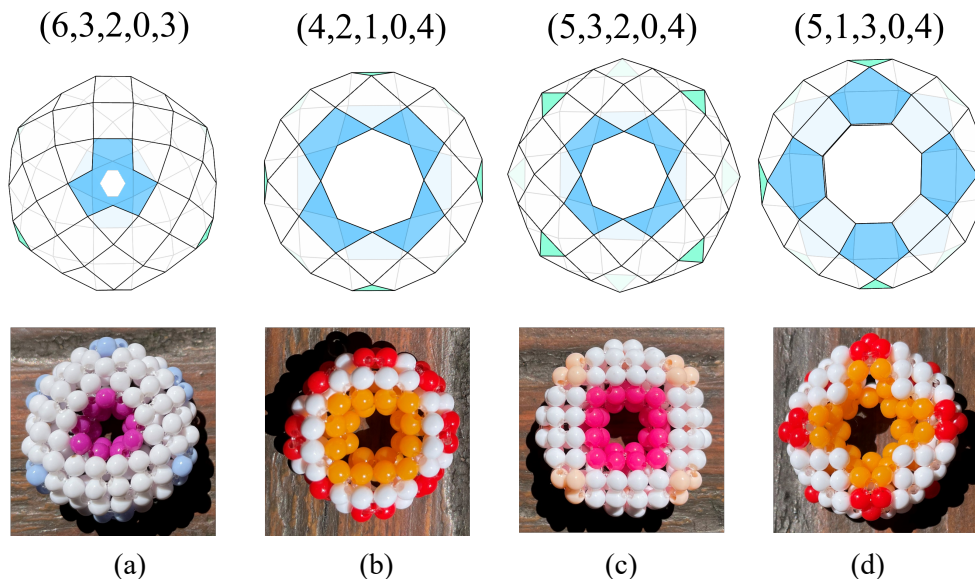


**Figure 5:** 3D images and bead models of tetravalent toroidal polyhedra with indices (a)  $(6,3,2,0,3)$ , (b)  $(4,2,1,0,4)$ , (c)  $(5,3,2,0,4)$ , and (d)  $(5,1,3,0,4)$ .

### Acknowledgements

We thank the Ministry of Science and Technology, Taiwan for financial support.

### References

- [1] C. Chuang, Y. C. Fan, and B. Y. Jin. “Generalized Classification Scheme of Toroidal and Helical Carbon Nanotubes.” *J. Chem. Inf. Model*, 2009, 49, 361-368.
- [2] D. Fujita, Y. Ueda, S. Sato et al. “Self-assembly of Tetravalent Goldberg Polyhedra from 144 Small Components.” *Nature*, 2016, 540, 563-566.
- [3] H. H. Ho, C. Chuang, and B. Y. Jin. “Constructing Bead Models of Smoothly Varying Carbon Nanotori with Constant Radii and Related Intersecting Structures” *Bridges Conference Proceedings*, Aug. 1–3, 2021, pp. 331–334.  
<https://archive.bridgesmathart.org/2021/bridges2021-331.html>
- [4] H. H. Ho and B. Y. Jin. “Orderly Branched Tangles Based on Carbon Nanotube Inspired by Grossman’s Sculptures” *Bridges Conference Proceedings*, Helsinki and Espoo, Finland, Aug. 1–5 2022, pp. 323–326.  
<http://archive.bridgesmathart.org/2022/bridges2022-323.html>
- [5] B. Y. Jin. *Chiral Cube – the Generalized Goldberg Polyhedra*  
<http://thebeadedmolecules.blogspot.com/2011/02/chiral-cube-generalized-goldberg.html>
- [6] T. Tarnai, F. Kovács, P. W. Fowler and S. D. Guest. “Wrapping the Cube and Other Polyhedra” *Proc. R. Soc. A*, 2012, 468, 2652-2666.